

Electronic Supporting Information

Enzyme/Metal Free Quinoxaline Assemblies: Direct Light-up Detection of Cholesterol in Human Serum

Amrit Kaur, Manoj Kumar* and Vandana Bhalla *

Department of Chemistry, UGC Sponsored Centre for Advanced Studies, Guru Nanak Dev University, Amritsar 143005, Punjab, India

mksharmaa@yahoo.co.in vanmanan@yahoo.co.in

Page No.

S3-4 Table S1 Comparison with recent literature reports.

S5 Instruments and experimental procedures

S6 Powder X-Ray Diffraction Sample preparation details and Synthetic route and characterisation of **QxPyA**

S7 Synthetic route and characterisation of **QxP**.

S8 Synthesis and characterisation of **QxTPY**

S9 The ^1H NMR of **QxPyA** in CDCl_3 and The ^{13}C NMR of **QxPyA** in CDCl_3 at 500 MHz.

S10 HRMS Mass spectra of **QxPyA**.

S11 The ^1H NMR and ^{13}C NMR of **QxP** in CDCl_3 at 400 MHz.

S12 The ^1H NMR of **QxTPY** at 500 MHz and The ^{13}C NMR in CDCl_3 at 400 MHz of **QxTPYP**

S13 Cyclic voltammogram of **QxPyA** under N_2 saturated ACN. The potential was scanned at 100 mV s^{-1} using glassy carbon (working); Ag/AgCl (reference) and platinum wire (counter) electrode with (0.1M) tetrabutyl ammonium hexafluorophosphate (TBAPF) as supporting electrolyte in ACN and The absorption spectra and fluorescence spectra of **QxPyA** ($10 \mu\text{M}$) in various solvent of different polarity at room temperature at $\lambda_{\text{ex}} = 375 \text{ nm}$ Inset showing the fluorescence of **QxPyA** in different solvent upon illumination under UV lamp

S14 The fluorescence spectra of **QxPyA** ($10 \mu\text{M}$) showing change in emission intensity upon increasing temperature from $25 \text{ }^\circ\text{C}$ - $75 \text{ }^\circ\text{C}$ in acetonitrile at $\lambda_{\text{ex}} = 375 \text{ nm}$ and The time-resolved fluorescence spectra of **QxPyA** ($10 \mu\text{M}$) in DMSO and MeOH at $\lambda_{\text{ex}} = 377 \text{ nm}$.

S15 The fluorescence spectra **QxPyA** ($10 \mu\text{M}$) upon varying % volume fraction of glycerol in DMSO (0 to 99, v/v) at $\lambda_{\text{ex}} = 375 \text{ nm}$ and The absorption spectra of **QxPyA** ($10 \mu\text{M}$) upon varying % volume fraction of water in (f_w) DMSO (0 to 99, v/v)

S16 The fluorescence spectra of **QxPyA** (10 μM) upon varying water of fraction (f_w) in DMSO (0 to 99) at $\lambda_{\text{ex}} = 375$ nm, (b) fluorescence emission spectra of **QxPyA** in 40% and 99% H_2O in DMSO and The SEM (scale 500 nm) of aggregates of **QxPyA** in 99% H_2O in DMSO (b) The DLS studies of **QxPyA**(10 μM) in 99% H_2O in DMSO having particles of size ~ 48.5 nm and ~ 220 nm.

S17 The PXRD pattern of **QxPyA** (blue) assemblies and (b) **QxPyA** assemblies after addition of cholesterol (pink) and The absorption spectra of **QxPyA** (10 μM) upon addition of cholesterol (0-6.0mM) in 99% H_2O in DMSO

S18 The fluorescence response of **QxPyA** (10.0 μM) to various concentrations of cholesterol in 99% H_2O in DMSO at $\lambda_{\text{ex}} = 375$ nm.

S19 The fluorescence emission response for **QxPyA** in aqueous medium in presence of cholesterol and various interfering analytes (6.0 mM) and The fluorescence emission response for **QxPyA** (10.0 μM) in 99% H_2O in DMSO in presence of cholesterol and various competitive interfering analytes at $\lambda_{\text{ex}} = 375$ nm

S20 The time-resolved fluorescence spectra curve of **QxPyA** (10 μM) upon addition of Cholesterol (6.0 mM) in 99% H_2O in DMSO at $\lambda_{\text{ex}} = 377$ nm and DLS studies of **QxPyA** in presence of cholesterol

S21 The ^1H NMR Spectrum of **QxPyA** in $\text{DMSO-d}_6:\text{D}_2\text{O}:\text{CD}_3\text{OD}$ (9.0:0.2:0.8, v:v:v) upon addition of Cholesterol (6.0 mM dissolved in $\text{DMSO-d}_6:\text{D}_2\text{O}:\text{CD}_3\text{OD}$ 9.0:0.2:0.8, v:v:v)

S22 The fluorescence spectra of **QxP** (10 μM) upon addition of cholesterol in 99% H_2O in DMSO at $\lambda_{\text{ex}} = 400$ nm and The fluorescence spectra of **QxCHO** (10 μM) upon addition of cholesterol (0-6.0) mM in 99% H_2O in DMSO $\lambda_{\text{ex}} = 375$ nm.

S23 The fluorescence emission spectra of **QxTPY** (10 μM) upon addition of cholesterol (0-6.0 mM) in 99% H_2O in DMSO at $\lambda_{\text{ex}} = 375$ nm. and The Fluorescence spectra of **QxPyA** for 200-fold dilution of human serum upon addition of cholesterol 6.0 mM in 99% H_2O in DMSO at $\lambda_{\text{ex}} = 375$ nm.

S24 References.

Table S1: Comparison with recent literature reports

S.No	Journal	Design	Detection Method	LOD	Response	Response strategy	Selectivity
1.	This work	Pyrazine based Supramolecular assemblies	Non enzymatic, increased π - π stacking.	4 nM	'turn on'	Non enzymatic, No External chromogenic substrate	Selective For cholesterol
2.	ACS Appl. Nano Mater. 2021 , <i>4</i> , 13612–13624	fluorescence resonance energy transfer (FRET)-based fluorescence "switch-off-on" of N-CQD (donor) and act as MnO ₂ nanowires (acceptor)	❖ Blocking of FRET in N-CQD composites by H ₂ O ₂ produced from the reaction of cholesterol oxidase in the presence of cholesterol. ❖ blocking of of FRET induces fluorescence recovery	4.89 nM	'turn on'	Enzymatic detection, External chromogenic substrate,	Non selective , detect biothiols, Acetyl cholinesterase, and Chlorpyrifos
3.	ACS Appl. Nano Mater. 2021 , <i>4</i> , 8282–8291	citric acid functionalized rhodium–platinum nanoparticles	❖ CA-RhPt NPs exhibited enhanced peroxidase-like activity that catalyzed the reaction between 3,3',5,5'-tetramethylbenzidine (TMB) and hydrogen peroxide (H ₂ O ₂) due to the synergistic effects of Rh and Pt. Enzyme	25.7 μ M	Absorbance based detection	Enzymatic detection, External chromogenic substrate	Selective For cholesterol
4.	ACS Appl. Mater. Interfaces 2021 , <i>13</i> , 3653–3668	Gold Nanoparticles on TiO ₂ Nanotubes	❖ Electrochemical new oxidation and reduction peak for both cholesterol and H ₂ O ₂	0.024-1.2 mM	-	Non-enzymatic (cyclic voltametric potential change)	Non selective , Detect H ₂ O ₂ and cholesterol
5.	ACS Appl. Nano Mater. 2021 , <i>4</i> , 9132–9142	ZIF-8 framework, the Pd nanoclusters	❖ Pd@ZIF 8 mimics peroxidase enzyme activity ❖ TMB Converted to TMBDI , Thiamine to (non-fluorescent) Thiochrome (fluorescent) by H ₂ O ₂	0.092 μ M	'turn on'	Enzymatic detection Concentration of H ₂ O ₂ produced related to concentration of cholesterol, External chromogenic substrate	Non selective , Detect glucose and cholesterol

6.	ACS Sustainable Chem. Eng. 2020 , <i>8</i> , 9404–9414	metal-free 2(3),9(10),16(17), 23(24)-octamethoxyphthalocyanine (Pc(OH) ₈)	<ul style="list-style-type: none"> ❖ Phthalocyanine derivative mimics with enhanced peroxidase activity ❖ Enzyme Cholesterol oxidase that catalyses conversion of cholesterol to cholest-en-3-one and H₂O₂ ❖ H₂O₂ oxidises dye TMB to ox TMB 	0.1–0.9 mM		Enzymatic, Colorimetric, Concentration of H ₂ O ₂ indirectly used to measure cholesterol, External chromogenic substrate	Selective For cholesterol
7.	ACS Appl. Mater. Interfaces 2019 , <i>11</i> , 27233–27242	Plasmonic nanohybrid system (Bio@AgNPs)	<ul style="list-style-type: none"> ❖ Cholesterol oxidase producing H₂O₂ ❖ The generated H₂O₂ will cause etching of AgNP characteristic SPR Band observed 	5.50 μM		Enzymatic detection, External chromogenic substrate	Non selective, Detect glucose, cholesterol and H ₂ O ₂
8.	ACS Appl. Mater. Interfaces 2022 , <i>14</i> , 428-438	LiErF ₄ :0.5%Tm ³⁺ @LiYF ₄ upconversion nanoparticle fabricated with poly(methyl methacrylate) (PMMA) photonic crystals (OPCs)	<ul style="list-style-type: none"> ❖ Generation of H₂O₂ in the Presence of O₂/cholesterol by cholesterol oxidase (ChOx). ❖ Oxidation of TMB Which causes quenching of fluorescence of nanoparticle turning from red to blue. 	1.6 μM	'turn on'	Enzymatic detection, External chromogenic substrate,	
9.	J. Mater. Chem. C, 2019 , <i>7</i> , 12674	β-cyclodextrin (b-CMCD) was grafted onto the LMOF,	<ul style="list-style-type: none"> ❖ Porous MOF, ❖ encapsulated Rh6G in Hydrophobic and porous cavity of Cyclodextrin based MOF, ❖ Displacement of Dye by cholesterol 	0.092 μM	'turn on'	Non-enzymatic, Porosity and hydrophobic effect (Displacement), External chromogenic substrate	Selective for cholesterol
10.	ACS Omega 2019 , <i>4</i> , 9333–9342	Inner filter effect based detection between nitrogen, cobalt co-doped carbon dots (N,Co-CDs) with 2,3-diaminophenazine (DAP)	<ul style="list-style-type: none"> ❖ The inner filter effect between N,Co-CDs and DAP result in ratiometric response. ❖ DAP is generated From Orthophenylene diamine after reaction with H₂O₂ produced as enzyme catalysed oxidation product of cholesterol and uric acid by 	3.6 nM	'turn-on'	Enzymatic detection, External chromogenic substrate,	Non selective ' Detect cholesterol and uric acid

Instruments and experimental procedures:

Instruments

All the reagents and solvent for synthesis were purchased from Aldrich and used without further purification. For the photophysical studies the HPLC grade dried DMSO was used as a solvent. The UV-vis spectra was recorded using with SHIMADZU UV-2450 spectrophotometer, with quartz cuvette (path length =1 cm), with cell holder thermostated at 25° C. The fluorescence spectrum was recorded using HORIBA Fluoromax-4 systems. The time-resolved fluorescence spectra were recorded with a HORIBA time-resolved fluorescence spectrometer. The dynamic light scattering (DLS) measurements were made using a light scattering apparatus (Zetasizer, Nanoseries, Nano-ZS, Malvern Instruments). The HR-TEM images was recorded from High Resolution Transmission Electron Microscope (HR-TEM) - JEOL Jem 2100 Plus. The CV measurements was performed using Autolab PGSTAT302N Metrohm workstation using a glass cell with a three-electrode assembly comprising a platinum counter electrode and a glassy carbon electrode as the working electrode. Ag/AgCl was used as the reference electrode. The ¹H and ¹³C NMR experiments were recorded by using Bruker AVANCE IIIHD 500 MHz and JEOL 400MHz spectrophotometer in CDCl₃ and DMSO -d₆ as solvent and tetramethylsilane, SiMe₄ as internal standard. Data are reported as follows: chemical shifts in ppm, multiplicity (s= singlet, br= broad, t= triplet, multiplet= m, J= coupling constant represented in Hz. The column chromatography for purification was done using silica gel (60-120 mesh).

UV-Vis and Fluorescence studies:

For the UV-vis and fluorescence titration the 10⁻³M stock of **QxPyA** was prepared in the DMSO. The cholesterol stock was prepared by dissolving 4 mg cholesterol in 1ml ethanol and further serial diluted in distilled water for setting appropriate concentration. The 10 μM concentration of **QxPyA** was for each titration. The other interfering analyte (glucose, galactose, sucrose, mannose, fructose, urea, uric acid, ascorbic acid, glutathione, cysteine, alanine, dopamine, creatinine, serine, arginine, valine, histidine, tryptophan, phenylalanine, glutamic acid, Na⁺, K⁺, Ca²⁺ and Mg²⁺ ions) the standard solution (1M stock) was prepared and appropriate concentration 0-6.0 mM were added to record the spectra. In titration experiments, each time a 3 ml solution of **QxPyA** (30 μl probe in 2970 μl distilled water) was filled in a quartz cuvette (path length, 1 cm) and spectra were recorded after the addition of

appropriate analyte. For the detection of cholesterol in the human serum samples, the samples were pretreated with ethanol for deproteinization.¹ Before detection, the serum samples were diluted ten times with ethanol. Further, the calibration method was used to find the concentration.²

Calculation for Quantum Yield:

The quantum yield was calculated using integrated sphere.

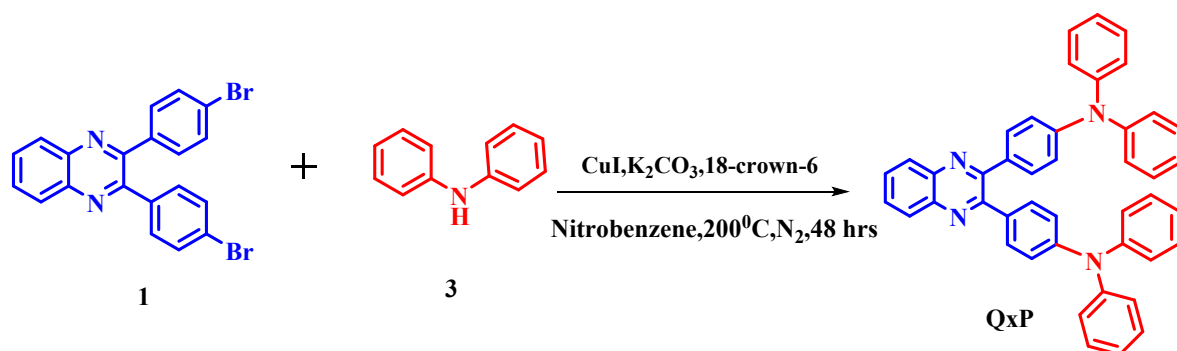
Powder X-Ray Diffraction (PXRD) Sample Preparation Details:

The 10mg compound **QxPyA** was dissolved in 99% H₂O in DMSO, the mixture was stirred at room temperature for 4-6 hrs. The aqueous solution was slowly evaporated and precipitate were filtered and dried for PXRD analysis. For the PXRD analysis in presence of 2M cholesterol (386.5 mg dissolved in 500 μ l ethanol) was added to the 99% H₂O in DMSO solution of compound **QxPyA**. The **QxPyA**:Cholesterol mixture was stirred at room temperature for 4-6 hrs, after the evaporation of aqueous solution the precipitates were filtered and dried for further analysis.

Synthetic route and characterisation of QxPyA:

To the solution of 2,3-bis(4-bromophenyl)quinoxaline **1** (0.30 g, 0.68 mmol) and 2,2'-dipyridylamino **2** (0.27 g, 2.5 mmol) and K₂CO₃ (0.28 g, 0.2 mmol) in 4 ml of dry nitrobenzene was stirred under nitrogen for 30 min. The reaction mixture was degassed three times followed by addition of CuI (0.27 g, 0.03 mmol) and 18-crown-6 in catalytic amount under inert atmosphere. The reaction mixture was refluxed at 200 °C for 48 hrs under nitrogen. After completion of the reaction (TLC), the reaction mixture was treated with water. The aqueous layer was extracted with ethyl acetate (3 X 10 mL). The combined organic layer was dried over anhydrous sodium sulphate and then distilled under reduced pressure to give a solid residue. The desired product was isolated by column chromatography using ethyl acetate/hexane (95/5) as an eluent and finally the product was recrystallized from hexane to give pure compound in 63% yield as light brown solid, m.p. 250-252 °C. The ¹H NMR (500 MHz, CDCl₃), δ (ppm) = 8.33 (br, 4H), 8.17-8.15 (m, 2H), 7.77-7.76 (m, 2H), 7.60 (d, *J*=10 Hz, 4H), 7.55 (t, *J*=15 Hz, 4H), 7.17 (d, *J*=10 Hz, 4H), 7.00 (d, *J*=5 Hz, 4H), 6.96 (t, *J*=15 Hz, 4H). ¹³C NMR (125 MHz, CDCl₃) δ (ppm) = 158.0, 152.71, 148.70, 145.87, 141.18, 137.77, 135.59, 131.25, 129.96, 129.15, 126.05, 118.67, 117.55. HRMS: (m/z) [M+H]⁺ calculated for [C₄₀H₂₉N₈]⁺ is 621.2509 found: 621.2518.

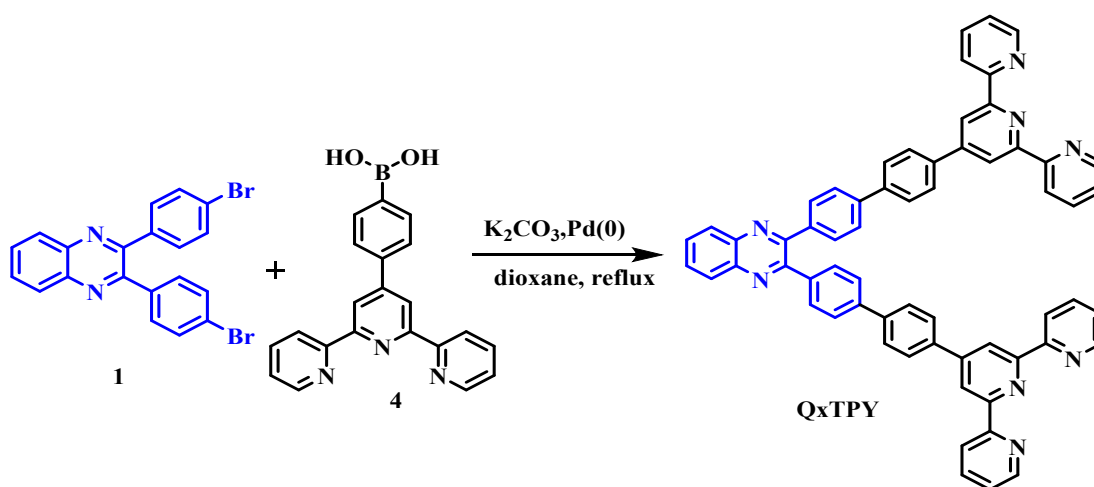
Synthetic route and characterisation of QxP



Scheme. S1 The synthetic route for QxP

Synthesis of QxP: To the solution of 2,3-bis(4-bromophenyl) quinoxaline **1** (0.30 g, 0.68 mmol) and diphenylamine **3** (0.28 g, 2.5 mmol) and K₂CO₃ (0.30g, 0.2 mmol) in 4 ml of dry nitrobenzene was stirred under nitrogen for 30 min. The reaction mixture was degassed three times followed by addition of CuI (0.27 g, 0.03 mmol) and 18-crown-6 in catalytic amount under inert atmosphere. The reaction mixture was refluxed at 200°C for 48 h under nitrogen. After completion of the reaction (TLC), the reaction mixture was treated with water. The combined organic layer was dried over anhydrous sodium sulphate and then distilled under reduced pressure to give a solid residue. The desired product was isolated by column chromatography using Chloroform/hexane (45/55) as an eluent and finally the product was recrystallized from hexane and ethyl acetate to give pure compound in 55% yield as yellow solid. The ¹H NMR (400 MHz in CDCl₃) δ (ppm) = 8.14-8.12 (m, 2H), 7.74-7.71 (m, 2H), 7.45 (d, *J*=8Hz, 4H), 7.29-7.25 (m, 8H), 7.14 (d, *J*=8 Hz, 8H), 7.09-7.03 (m, 8H). ¹³C NMR (100 MHz, CDCl₃) δ (ppm) = 153.22, 148.51, 147.31, 141.08, 132.54, 130.78, 129.57, 129.36, 129.01, 124.97, 123.45, 122.18. The characterisation data corroborate with literature report.³

Synthetic route and characterisation of QxTPY:



Scheme S2. The synthetic route for QxTPY

The QxTPY synthetic procedure and characterisation is reported in literature.⁴

Synthesis of QxTPY: To a solution of 2,3-bis(4-bromophenyl) quinoxaline **1** (0.4 g, 0.90 mmol) and 4-(2,2',6',2''-terpyridine-4'-yl)phenyl boronic acid **4** (0.73 g, 2.07 mmol) in anhydrous dioxane (20 mL), 2 mL aqueous solution of K_2CO_3 (0.99 g, 7.2 mmol) was added followed by the addition of $[Pd(PPh_3)_4]$ (0.51 g, 0.45 mmol) as a catalyst under nitrogen atmosphere. The reaction mixture was refluxed overnight and dioxane was then removed under vacuum. The residue so obtained was treated with water and extracted with ethyl acetate three times, dried over anhydrous sodium sulphate. The solvent was removed under reduced pressure and compound was purified by column chromatography using ethylacetate/hexane (80/20) as an eluent to give 80% yield of the derivative QxTPY as white solid; 1H NMR (500 MHz, $CDCl_3$) δ (ppm) = 8.80 (s, 4H), 8.75 (d, $J = 5$ Hz, 4H), 8.69 (d, $J = 5$ Hz, 4H), 8.23 (d, $J = 10$ Hz, 2H), 8.03 (d, $J = 5$ Hz, 4H), 7.91-7.88 (m, 4H), 7.84-7.78 (m, 8H), 7.74 (d, $J = 10$ Hz, 4H), 7.67 (d, $J = 5$ Hz, 2H), 7.39-7.35 (m, 4H), ^{13}C NMR (100 MHz, $CDCl_3$) δ (ppm) = 156.33, 156.10, 149.26, 141.40, 140.90, 137.04, 130.57, 129.34, 128.55, 127.91, 127.70, 127.20, 123.96, 121.49, 118.79.

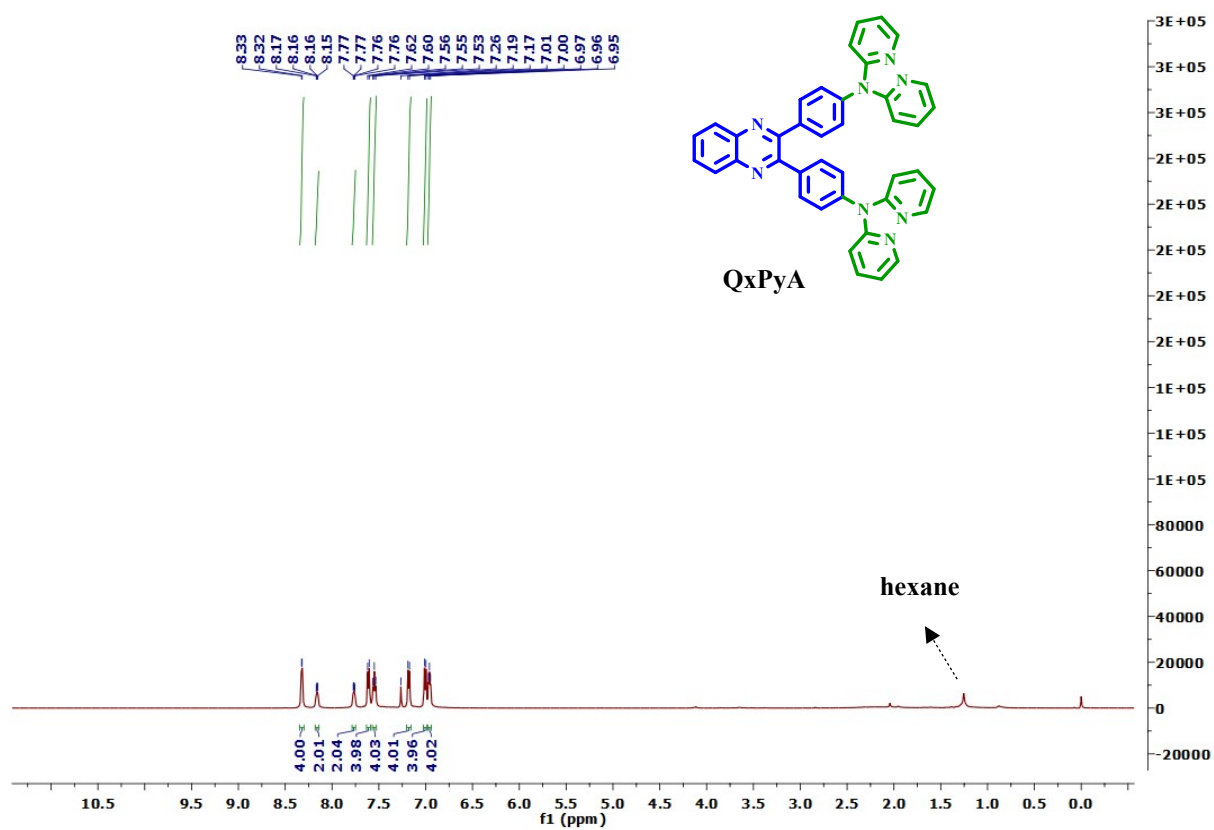


Fig. S1 The ^1H NMR of QxPyA in CDCl_3 at 500 MHz

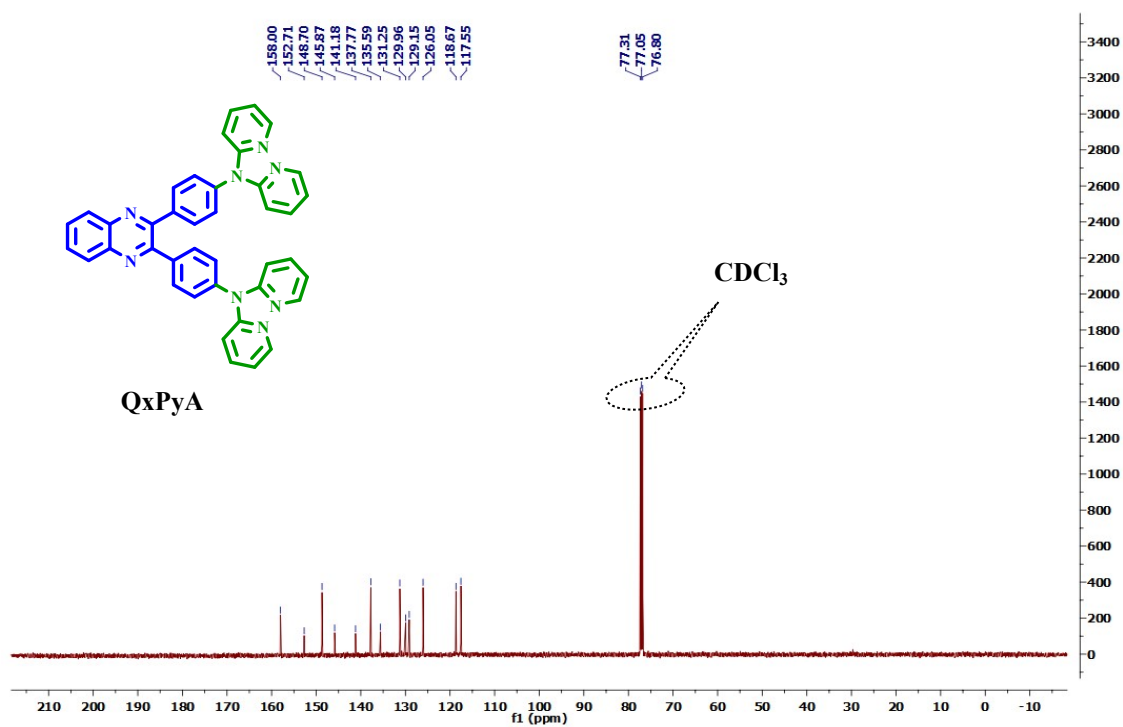
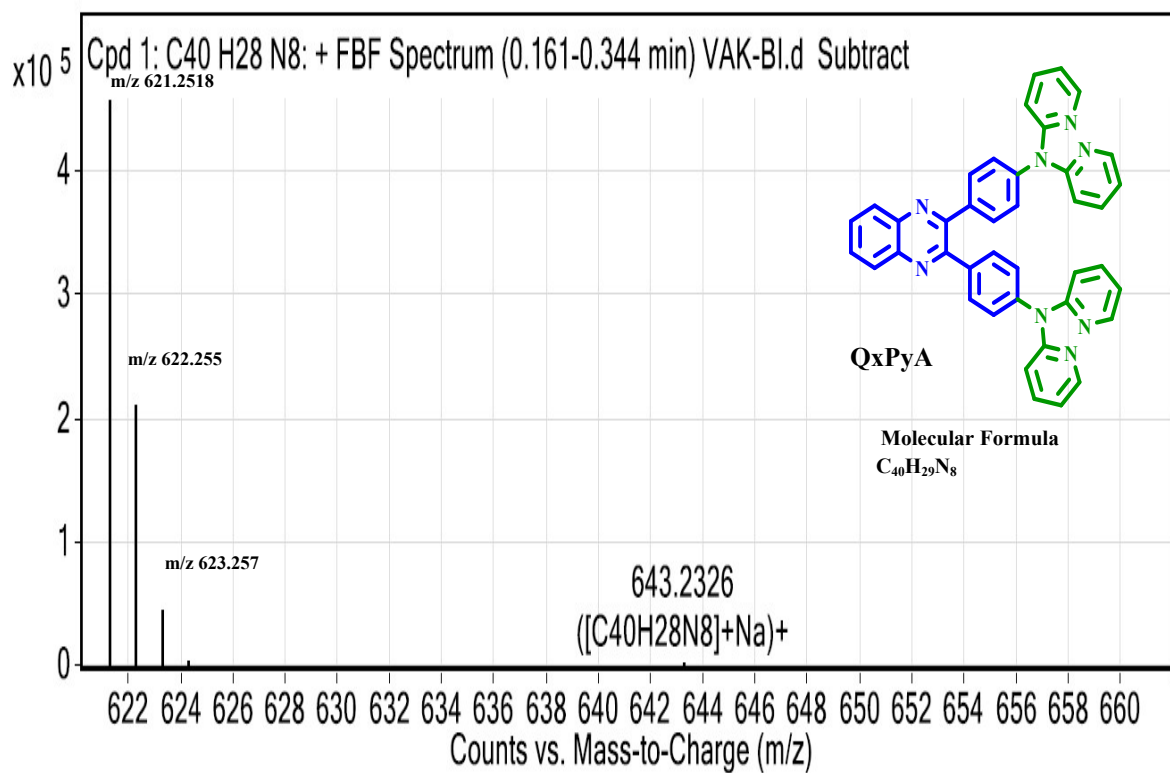


Fig. S2 The ^{13}C NMR of QxPyA in CDCl_3 at 500 MHz



Peak List

<i>m/z</i>	<i>z</i>	Abund	Formula	Ion
621.2518	1	459506.53	C ₄₀ H ₂₈ N ₈	(M+H) ⁺
622.255	1	212445	C ₄₀ H ₂₈ N ₈	(M+H) ⁺
623.257	1	47731.11	C ₄₀ H ₂₈ N ₈	(M+H) ⁺
624.2591	1	6107.88	C ₄₀ H ₂₈ N ₈	(M+H) ⁺
625.2647	1	862.36	C ₄₀ H ₂₈ N ₈	(M+H) ⁺
643.2326	1	4188.72	C ₄₀ H ₂₈ N ₈	(M+Na) ⁺
644.2351	1	2043.18	C ₄₀ H ₂₈ N ₈	(M+Na) ⁺
645.2418	1	648.25	C ₄₀ H ₂₈ N ₈	(M+Na) ⁺
659.2078	1	2443.57	C ₄₀ H ₂₈ N ₈	(M+K) ⁺
660.2119	1	1205.07	C ₄₀ H ₂₈ N ₈	(M+K) ⁺

Fig. S3 The HRMS Spectra of QxPyA

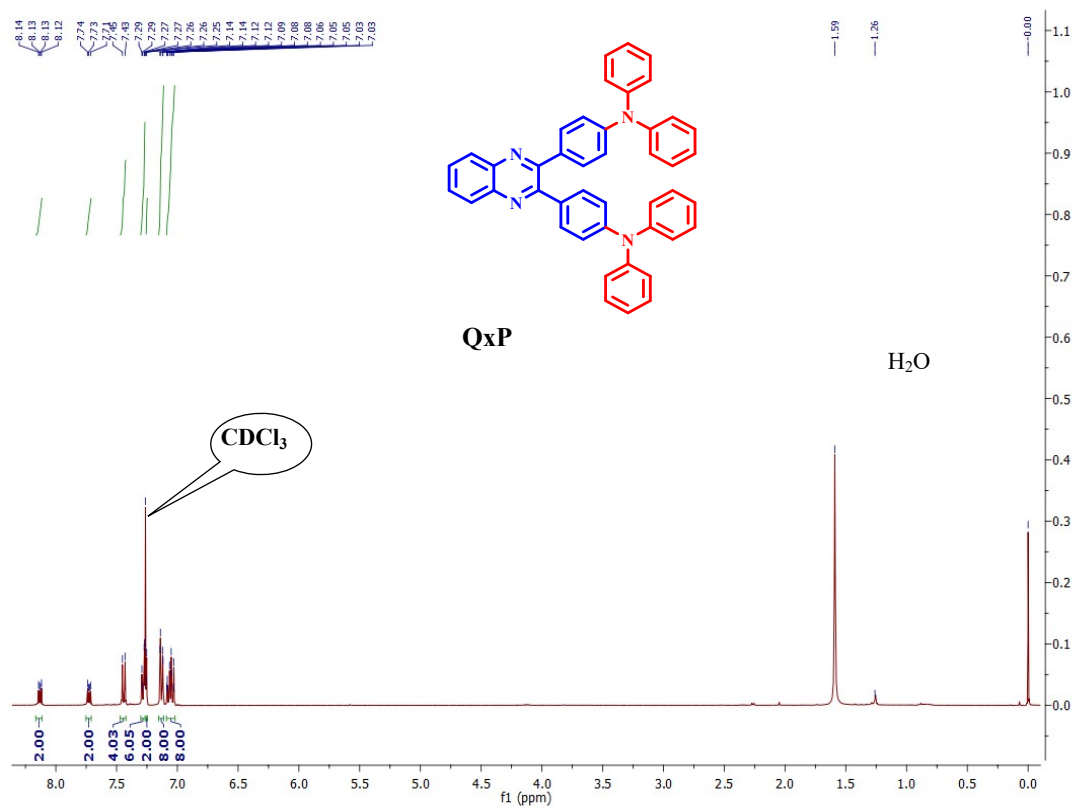


Fig. S4 The ¹H NMR of QxP in CDCl₃ at 400 MHz

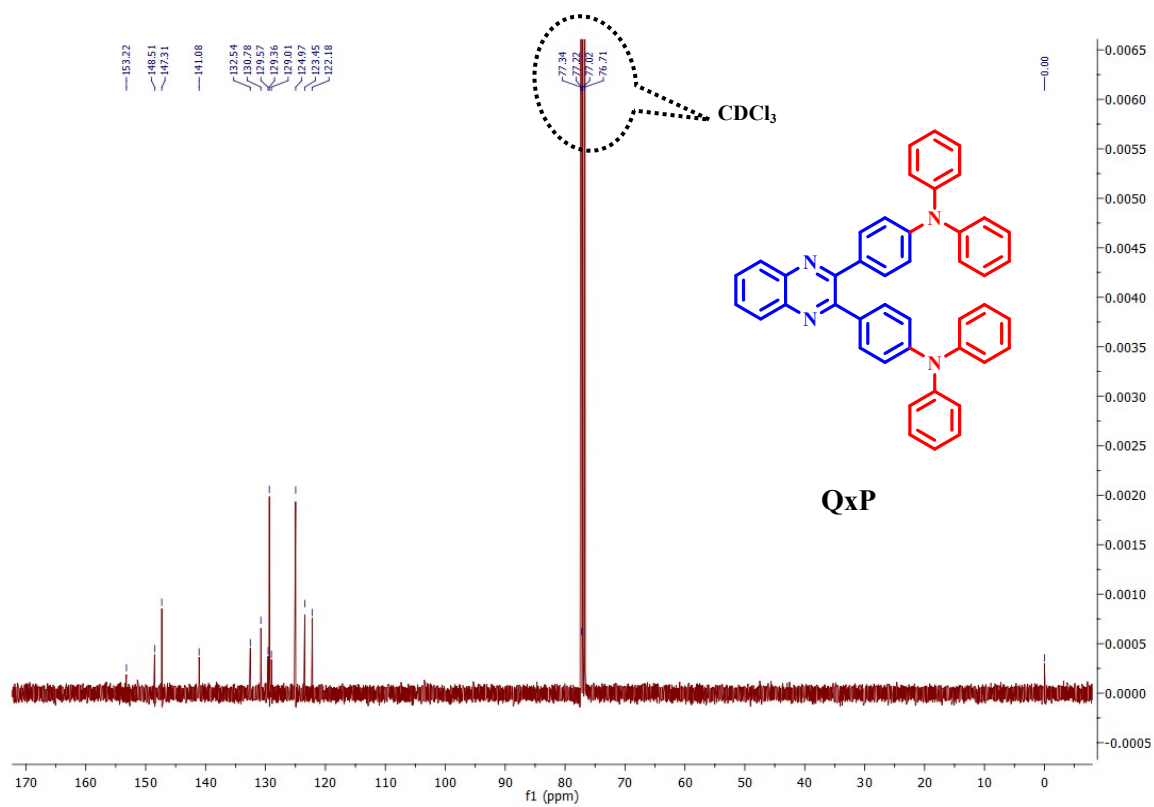


Fig. S5 The ¹³C NMR of QxP in CDCl₃ at 400 MHz

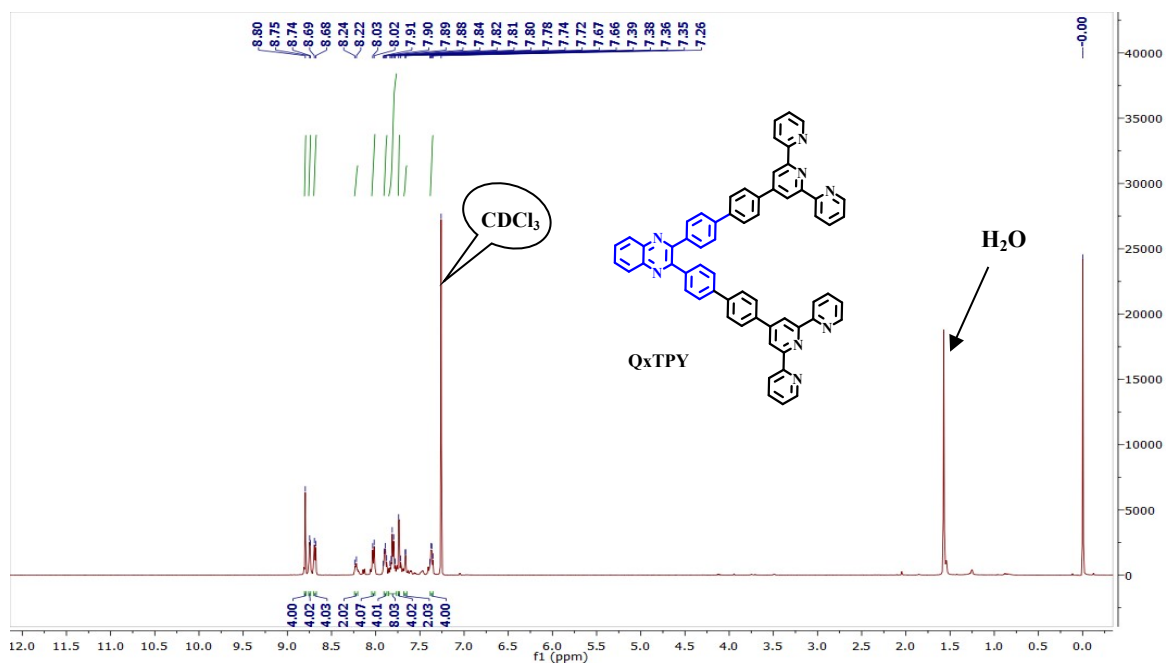


Fig S6. ¹H NMR Spectra of QxTPY in CDCl₃ at 500 MHz.

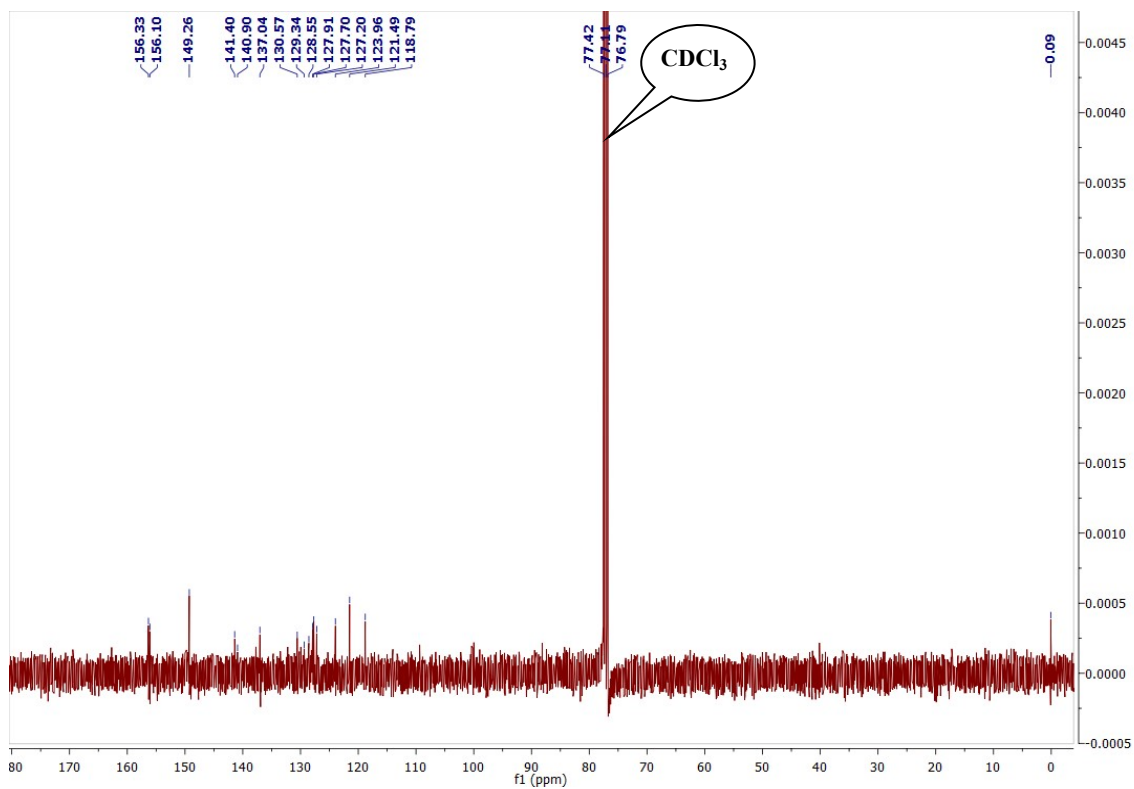


Fig. S7 ¹³C NMR Spectra of QxTPY in CDCl₃ at 400MHz.

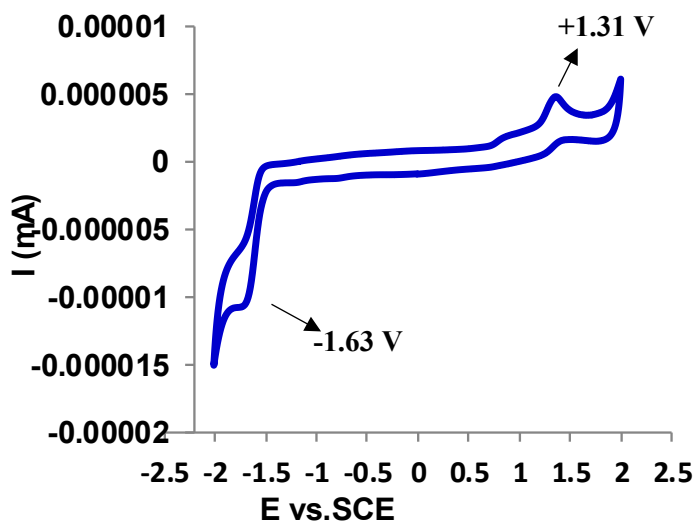


Fig S8 Cyclic voltammogram of **QxPyA** under N_2 saturated ACN. The potential was scanned at 100 mV s^{-1} using glassy carbon (working); Ag/AgCl (reference) and platinum wire (counter) electrode with (0.1M) tetrabutyl ammonium hexafluorophosphate (TBAPF) as supporting electrolyte in ACN.

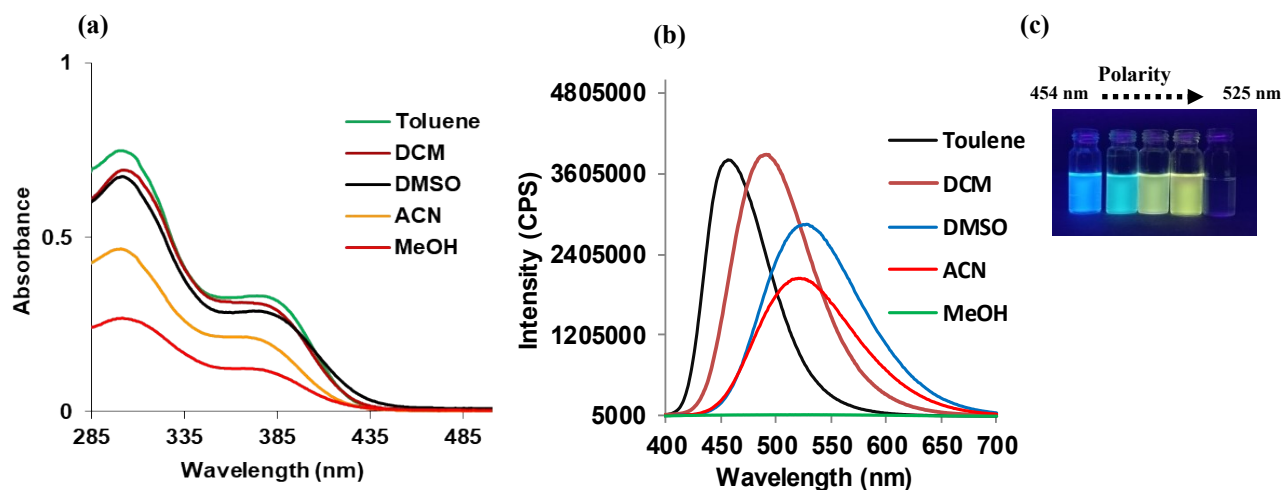


Fig. S9 (a) The absorption spectra and (b) fluorescence spectra of **QxPyA** ($10 \mu\text{M}$) in various solvent of different polarity at room temperature at $\lambda_{\text{ex}} = 375 \text{ nm}$ (c) Inset showing the fluorescence of **QxPyA** in different solvent upon illumination under UV lamp.

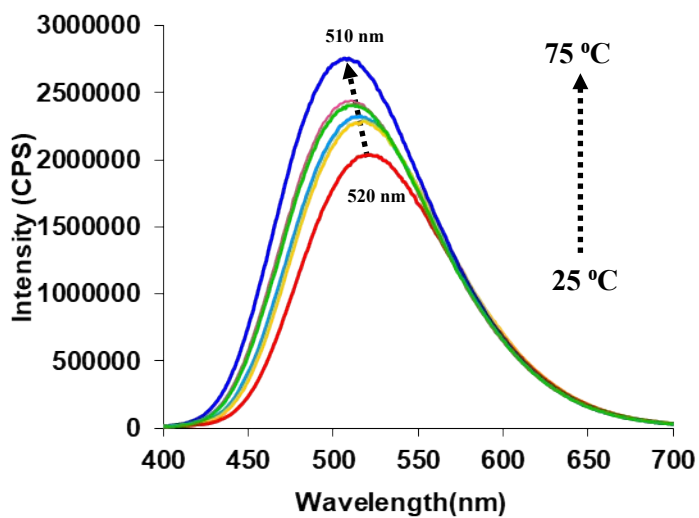


Fig. S10 The fluorescence spectra of QxPyA (10 μM) showing change in emission intensity upon increasing temperature from 25 °C-75 °C in acetonitrile at $\lambda_{\text{ex}} = 375$ nm.

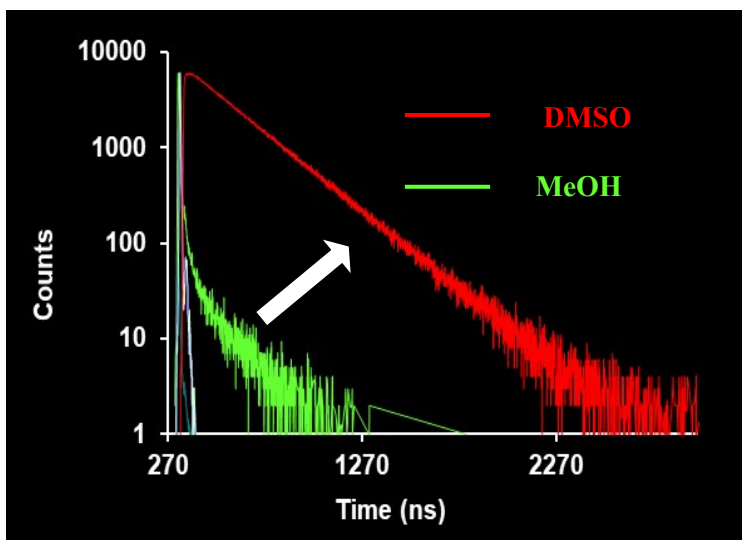


Fig. S11 The time-resolved fluorescence spectra of QxPyA (10 μM) in DMSO and MeOH at $\lambda_{\text{ex}} = 377$ nm.

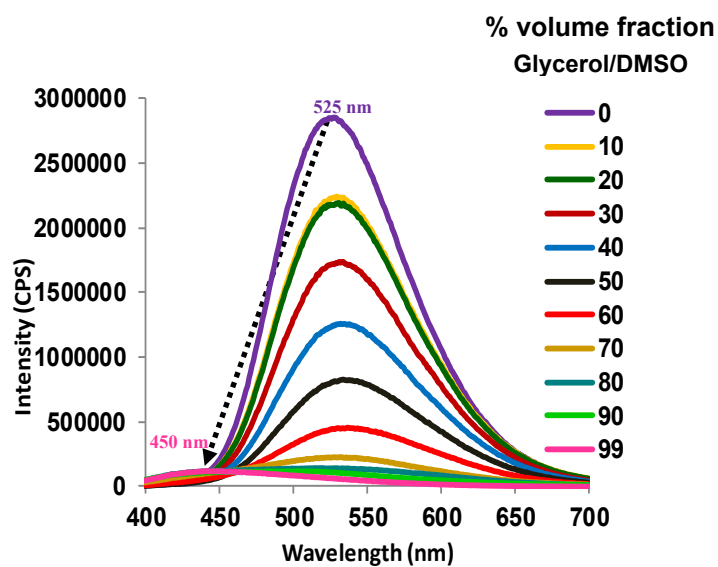


Fig. S12 The fluorescence spectra QxPyA (10 μM) upon varying % volume fraction of glycerol in DMSO (0 to 99, v/v) at $\lambda_{\text{ex}} = 375$ nm.

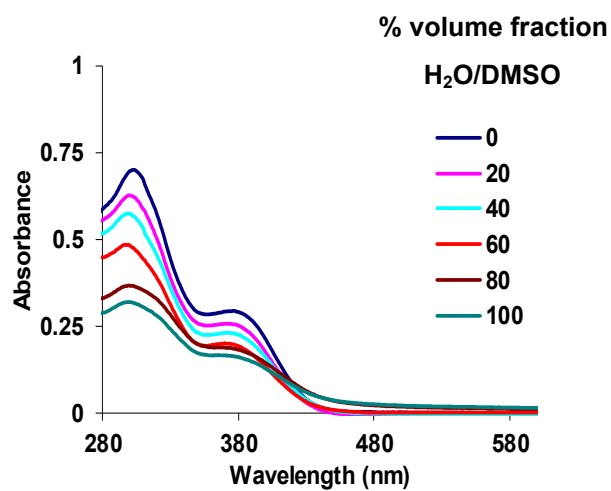


Fig. S13 The absorption spectra of QxPyA (10 μM) upon varying % volume fraction of water in (f_w) DMSO (0 to 99, v/v)

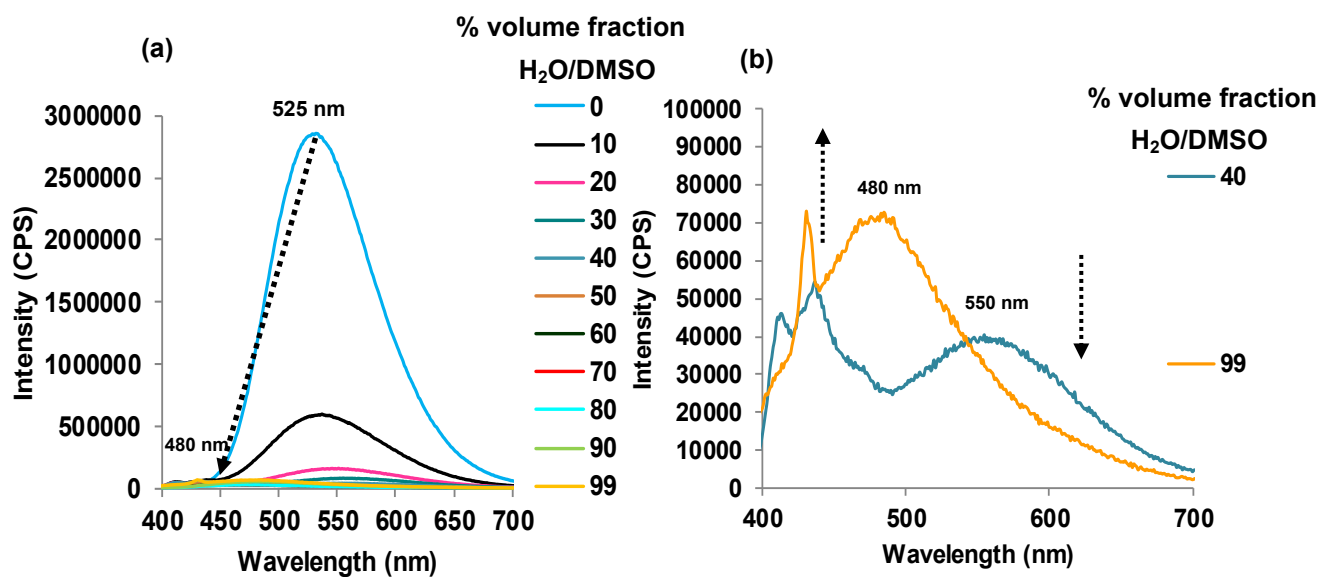


Fig. S14 The fluorescence spectra of QxPyA (10 μ M) upon varying water of fraction (f_w) in DMSO (0 to 99) at $\lambda_{ex} = 375$ nm, (b) fluorescence emission spectra of QxPyA in 40% and 99% H₂O in DMSO.

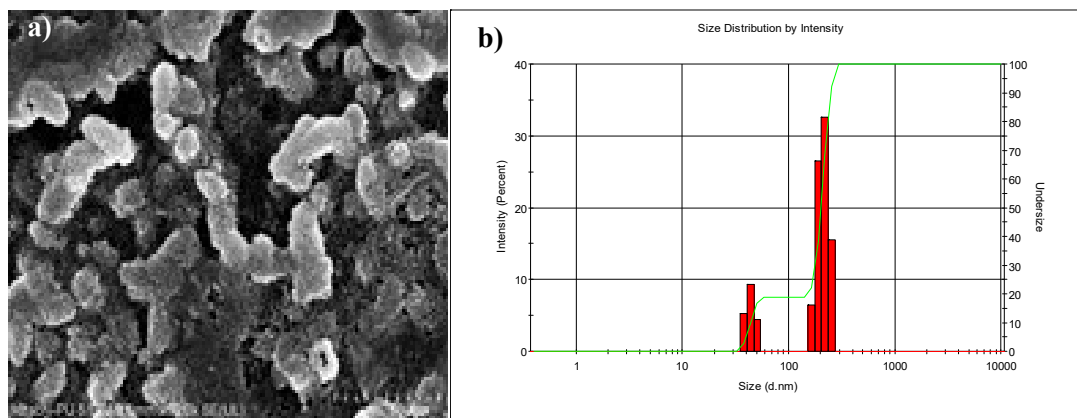


Fig. S15 (a) The SEM (scale 500 nm) of aggregates of QxPyA in 99% H₂O in DMSO (b) The DLS studies of QxPyA(10 μ M) in 99% H₂O in DMSO having particles of size \sim 48.5 nm and \sim 220 nm.

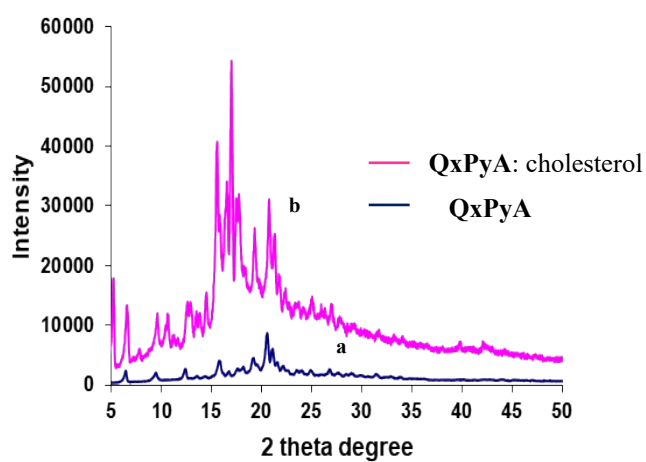


Fig. S16 (a) The PXR D pattern of QxPyA (blue) assemblies and (b) QxPyA assemblies after addition of cholesterol (pink).

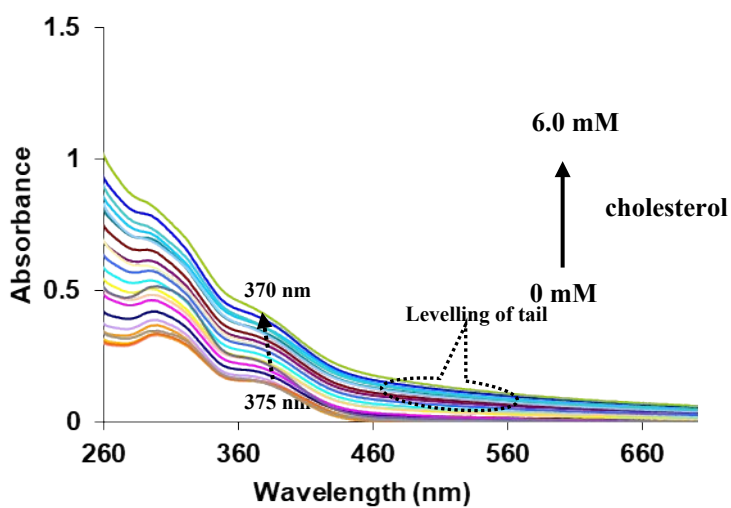


Fig. S17 The absorption spectra of QxPyA (10 μ M) upon addition of cholesterol (0-6.0mM) in 99% H₂O in DMSO.

Detection Limit Calculations of QxPyA for Cholesterol

The detection limit was calculated based on the fluorescence titration using strand calibration method.² To determine the S/N ratio, the emission intensity of QxPyA without Cholesterol was measured by 10 times and the standard deviation of blank measurements was determined. The detection limit is then calculated with the following equation: $DL = 3 \times SD/S$ Where SD is the standard deviation of the blank solution measured by 10 times; S is the slope of the calibration curve. From the graph, we get slope (S) = 6×10^6 , and SD value is 0.008 Thus using the formula we get the Detection Limit (DL) = 4 nM

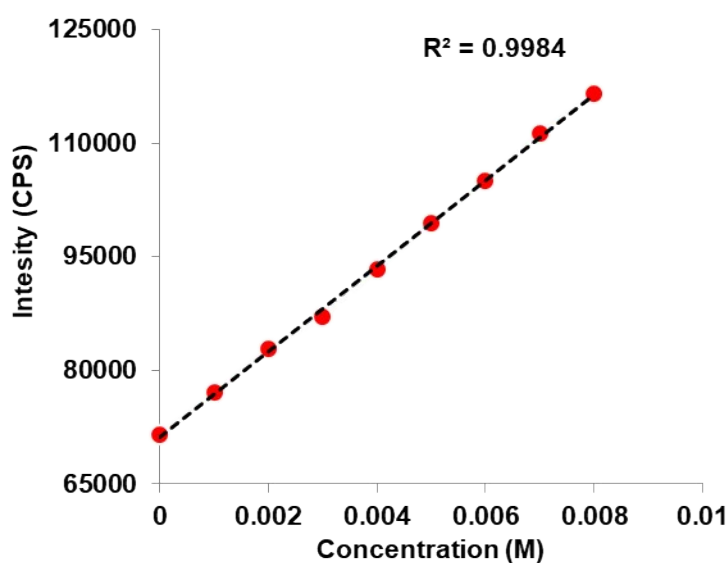


Fig. S18 The fluorescence response of QxPyA (10.0 μ M) to various concentrations of cholesterol in 99% H₂O in DMSO at λ_{ex} = 375 nm.

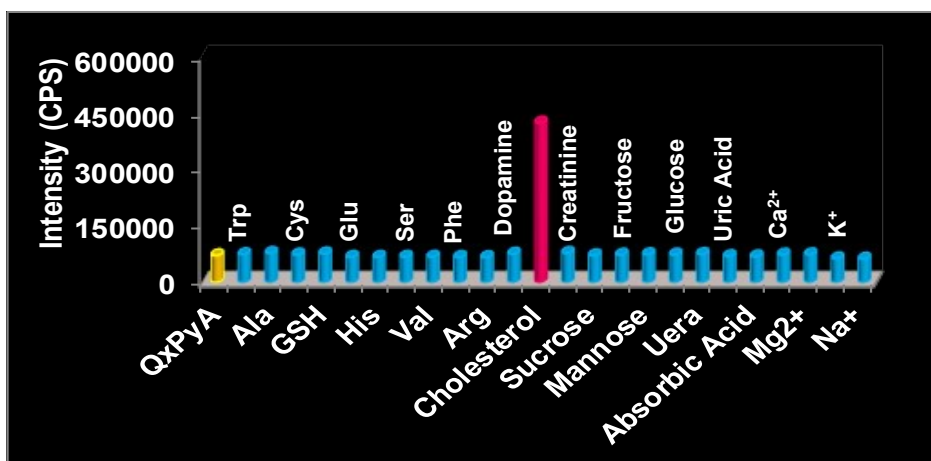


Fig. S19a The fluorescence emission response for QxPyA(10.0 μ M) in 99% H₂O in DMSO in presence of cholesterol and various interfering analytes 1. QxPyA , 2.Trp, 3. Ala,4. Cys, 5. GSH, 6. Gul, 7.His, 8. Ser, 9. Val, 10. Phe,11. Arg, 12. Dopamine, 13. Cholesterol, 14 Creatinine, 15. Sucrose, 16.Fructose, 17. Mannose,18. Glucose 19. Uera, 20. Uric acid, 21. Ascorbic acid, 22. Ca²⁺, 23. Mg²⁺, 24. K⁺, 25.Na⁺ (0 -6.0 mM)at λ_{ex} = 375

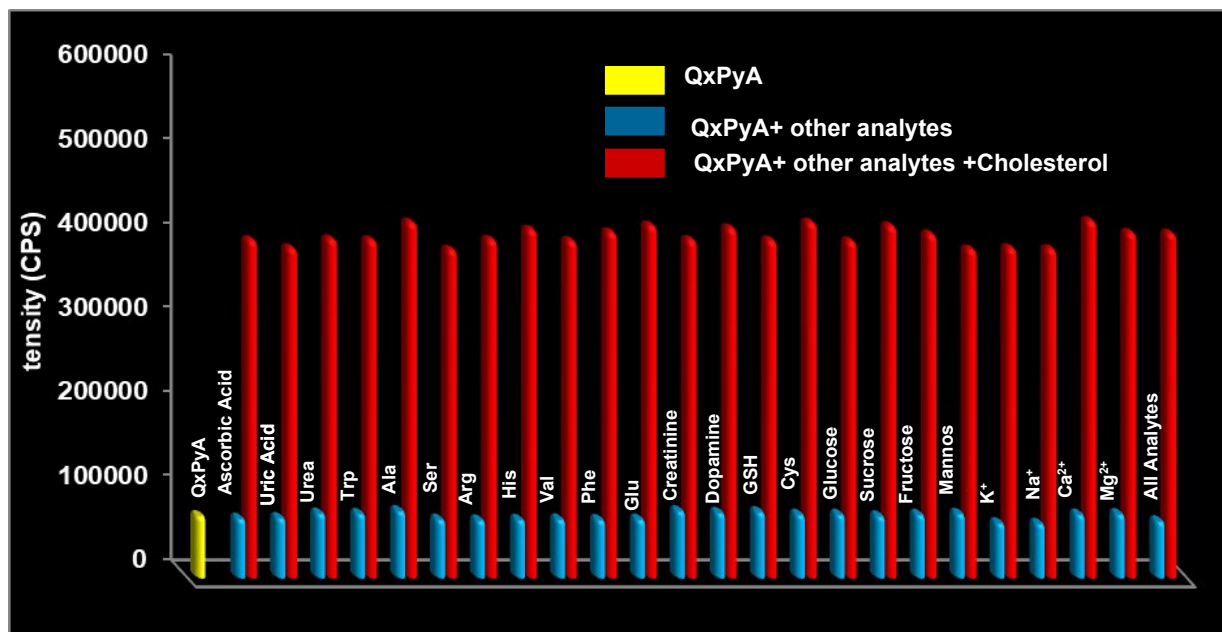


Fig. S19b The fluorescence emission response for QxPyA (10.0 μ M) in 99% H₂O in DMSO in presence of cholesterol and various competitive interfering analytes (0-6.0 mM)at λ_{ex} = 375 nm.

Na⁺

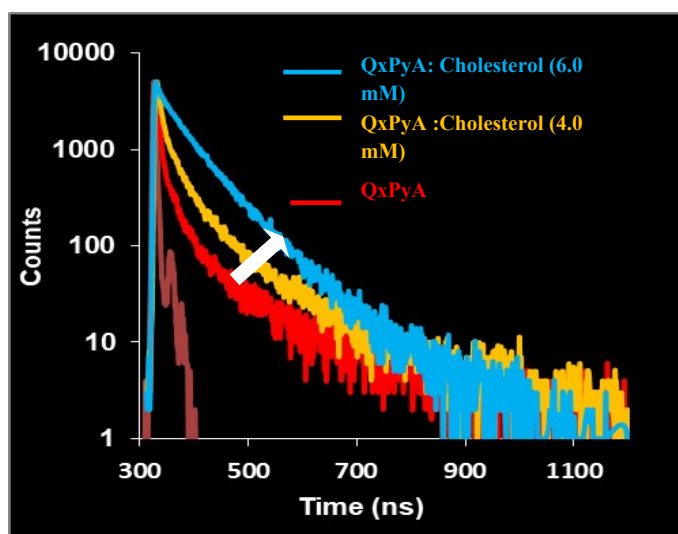


Fig. S20 The The time-resolved fluorescence spectra curve of QxPyA (10 μM) upon addition of cholesterol (6.0 mM) in 99% H_2O in DMSO at $\lambda_{\text{ex}} = 377 \text{ nm}$.

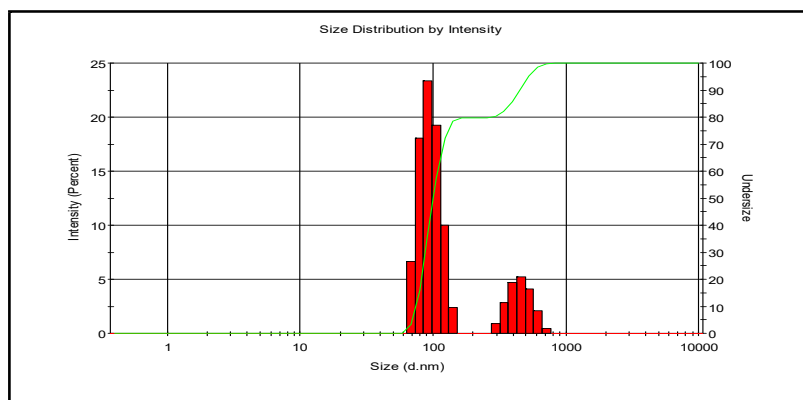


Fig. S21 The DLS studies of QxPyA (10 μM) showing increase particle size to $\sim 98.5 \text{ nm}$ and $\sim 458 \text{ nm}$ upon addition of cholesterol in 99 % H_2O in DMSO.

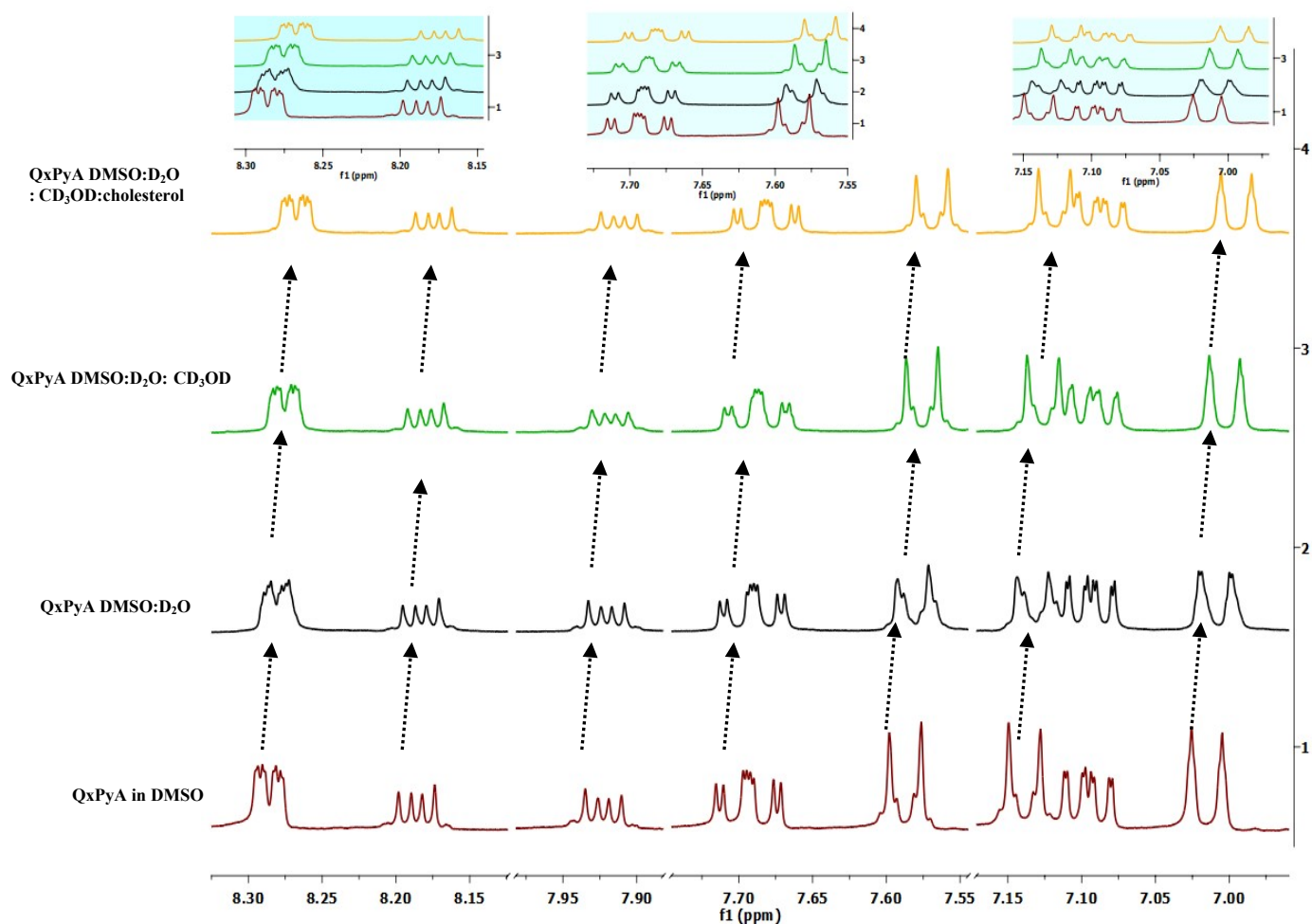


Fig. S22 The ^1H NMR Spectrum of QxPyA in DMSO- d_6 : D_2O : CD_3OD (9:0.2:0.8, v:v:v) upon addition of cholesterol (6.0 mM dissolved in DMSO- d_6 : D_2O : CD_3OD (9:0.2:0.8, v:v:v)).

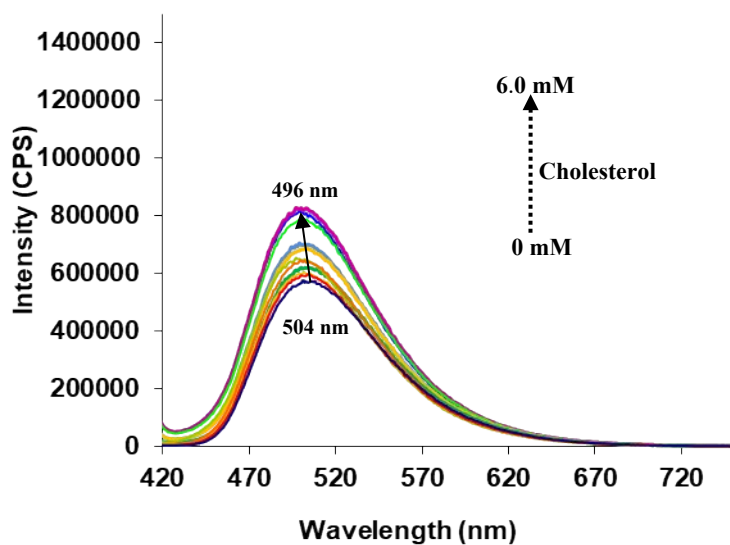


Fig. S23 The fluorescence spectra of **QxP** (10 μ M) upon addition of cholesterol (0-6.0 mM) in 99% H₂O in DMSO at λ_{ex} = 400 nm.

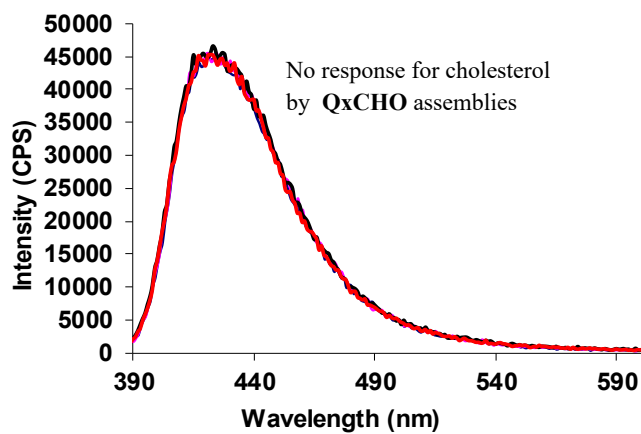


Fig. S24 The fluorescence spectra of **QxCHO** (10 μ M) upon addition of cholesterol (0-6.0 mM) in 99% H₂O in DMSO at λ_{ex} = 375 nm.

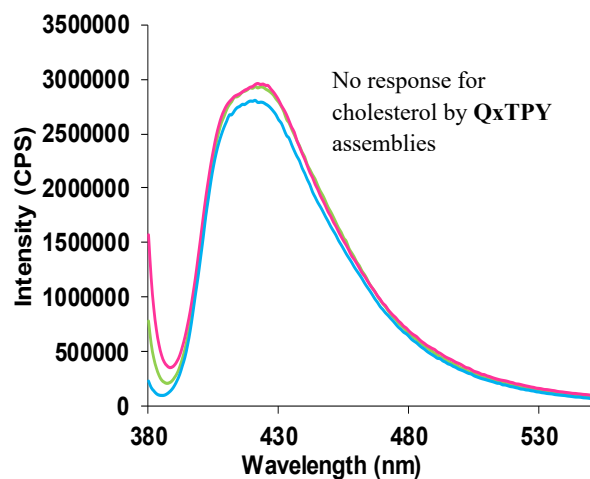


Fig. S25 The fluorescence spectra of QxTPY (10 μ M) upon addition of cholesterol (0-6.0 mM) in 99% H₂O in DMSO at λ_{ex} =375 nm.

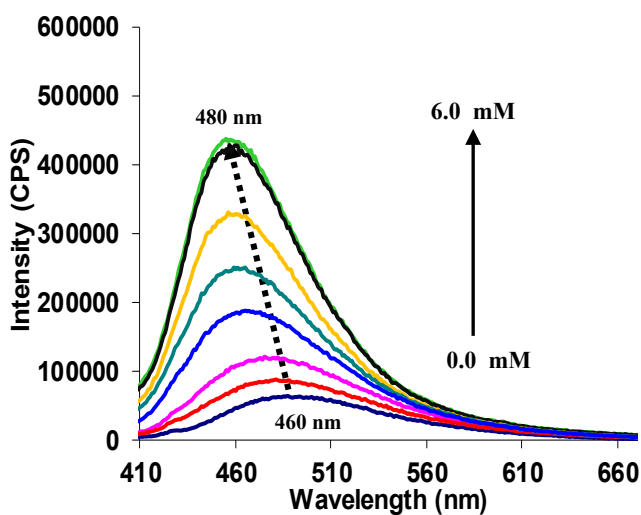


Fig. S26 The fluorescence spectra of QxPyA for 200-fold dilution of human serum upon addition of cholesterol 6.0 mM in 99% H₂O in DMSO at λ_{ex} =375 nm.

References:

1. a) R. J. Franey and E. Amador *Clin. Chim. Acta*, 1968, 21, 255-263. b) R. R. Burgess, *Methods Enzymol.*, 2009, **463**, 331-334.
2. L. Zeng, T. Chen, B. Zhu, S. Koo, Y. Tang, W. Lin, T.D. James and J.S. Kim, *Chem. Sci.*, 2022, **13**, 4523.
3. a) W. Wang, H. Chen, Y. Yue, R. Zhang and J. Liu, *Dyes Pigm.*, 2021, **194**, 109615. b) L. Xu, H. Zhu, G. Long, J. Zhao, D. Li, R. Ganguly, Y. Li, Q. H. Xu and Q. Zhang, *J. Mater. Chem. C*, 2015, **3**, 9191-919
4. S. Dadwal, H. Deol, M. Kumar, and V. Bhalla, *Sci. Rep.*, 2019, **9**, 11142.